Transient High Pressure Spray Cooling of Moving High Temperature Surfaces

Nasr G.G.[1], Sharief RA[2], Rho S[2], Yule A.J.[2]

1. School of Aeronautical, Civil and Mechanical Engineering, University of Salford, Manchester M5 4WT, England
2. Department of Mechanical, Aerospace and Manufacturing Engineering, UMIST, PO Box 88, Manchester M60 1QD, England

Abstract
Utilization of high pressure water in spray cooling of heated surfaces (up to 1300K) has been common practice in steel, copper, aluminium and metal powder production. Consistent mechanical and metallurgical properties in the alloys require an accurate surface temperature control during the process operation.
An experimental investigation has been performed with a vertically downwards spray impinging on a rotating still disk of a 250*mm* diameter at surface temperature up to 600 ^{o}C. Three full-cone atomizers with orifice diameters of 0.94-1.70*mm* were used, with the similar performances, reported previously by the authors Yule et al. [1]. Measurements were made at vertical distances of 140 and 240 mm from the atomiser tip to the test segment, using pressure up to 2.07 MPa and with the speed of the rotating disk 60 and 120 *rpm*, in order to study the effect of the following spray parameters on the cooling of the rotating disk surface: volume median drop diameter ($D_{v0.5}$), drop impinging velocity (U) and drop mass flux (G). The range of parameters considered is 0.98 to 12.5 kg m^{-2} s^{-1} for mass flux, 49.0 to 230.4 μm for volume median drop diameter and 9.8 to 32.3 m s^{-1} for impinging velocity. Correlation equations were derived to find relationships of heat flux with the spray parameters.

1. Introduction

Sprays have been used effectively to cool hot objects in many industrial processes because of their convenience of use and high heat dissipating ability. One of the major secondary processes carried out in the metallurgical industries is that of cooling. There is, however, a lack of collated information to provide better understanding of the hydrodynamic and thermodynamic behaviour of the spray droplets. In upstream steel manufacturing processes for example, continuous casting, descaling and hot rolling, knowledge of transient heat flux due to droplets, supported on the moving surface by vapour layers, is important in order to control overall production costs and at the same time maintaining the final product quality Nasr et al.[2]. At present the most common specific water-cooling methods in the steel industry for the above processes include: (a) relatively low pressure dilute sprays, positioned between mill rollers, to spray on both slabs and rollers in

Continuous casting and mill work rolls and (b) Laminar water cooling curtains and spray cooling, positioned between rolling stands in the hot strip mill: so-called inter-stand cooling, Nasr et al. [3]. Both methods can provide a non-ideal heat transfer process (e.g. inconsistent material properties, overheating rollers and excessive water consumption). Considerable experimental work has been carried out in this field for dilute sprays, rather than dense sprays, using low-pressure sprays or two-fluid atomization which has more restricted industrial applications, Choi et al. [4]. However, much more is desired in terms of quantitative information with regard to the spray parameters at high water pressure and their effects on the heat transfer characteristics of hot surfaces (about 1503*K*) in the film boiling regime. Water atomization involving a high velocity dense spray impacting on hot surfaces has a number of other applications, including in diesel engines and in metal powder production, Yule and Dunkley [6]. Previous studies have been carried out on steady state and transient conditions Choi et al.[4]; and Sharief et al.[5], i.e. where heat input is used to maintain a steady state surface temperature (about *1503 K*), or where the surface is allowed to cool during spraying, respectively. However, there is a lack of information on the fundamental mechanisms of heat transfer to an array of impacting drops under different surface conditions (material properties, surface roughness and surface temperature).

The main objectives of the present work are to study (a) the heat transfer characteristics of vertical sprays, with a range of densities, produced using full cone atomizers and impacting on a moving steel surface, for water supply pressure up to at least 2 MPa and for a range of exit orifice diameters (b) to study heat transfer using high-pressure water sprays and a rotating steel disk, with surface velocity up to 1.4 m/s and (c) to examine and correlate, the parametric effects of the mass flux, the drop size and impinging velocity, on heat transfer for temperature up to at least 600 ^{o}C.

2. Experimental Apparatus and Procedure

2.1 Overview

The transient cooling apparatus based upon the concept of a rotating disk, described previously in reference Nasr et al. [2], can meet the current general specifications of the inter-stand cooling process of the steel making industry. In practice, the strip is normally cooled down rapidly by, continuous laminar stream of water (a water curtain) which can, sometimes; provide inconsistent cooling along the hot moving surface when operated on its own, or water spray or a combination of both. The maximum strip speed and temperature reach 18 *m/s* and greater than 900 ^{o}C respectively. Thus the test apparatus could be able to meet the specifications of; (a) achieving high and uniform initial temperatures (over 900 ^{o}C), (b) obtaining the required strip speeds up to *18 m/s*, (c) with spray angles up to 45^{o} , simultaneously spraying bottom and top, and (d) accurately measuring the temperature drop as the surface passes through the spray. The spray angles can be related directly to the present conditions of the inter-stand cooling process where angle of the steel strip in the hot rolling mill is changed between 18-45^{o} with respect to the horizontal by a “looper”, which is installed between stands in order to maintain an appropriate strip tension.

2.2 Test Apparatus

Fig.1 shows the spray cooling test apparatus consists of a main frame constructed of tubular steel box section, a heating system, a spray system, a rotating disk and a data acquisition system. The main frame supported the hollow shaft on which was the rotating disk, the slip ring commutator, the motor and the burners. Its strength should endure the impact force of a spray, and should allow the possibility of being tilted without significant deformation occurring [2], to study the effects of heat transfer characteristics for different spray angles (for example 15°, 30° and 45°), and also for different angles of the disk surface (although these angular parameters were not tested here). Fig.2 shows the mild steel test segment which was tapered 10° and screwed into place so that it would not come loose due to centrifugal force when the disk was rotated. The test segment consists of two pieces, for convenience when welding thermocouples to the bottoms of their holes. There were nine holes on three planes to measure temperature differences between the thermocouples in order to derive heat fluxes in metal. However only six holes were used, due to insufficient input channels of the available data acquisition card. Each set of holes was staggered at around 45^{o} to minimise temperature distortion caused by having all three ceramic insulators in a vertical line. Mild steel was chosen for this research, because it is directly related to the product produced in the hot rolling process. The top surface of the test segment was directly exposed to the spray through a slot in a canopy (40mmx10mm). The characteristics of full cone sprays indicated that radial distributions of the mass flux, volume median diameter and average drop velocity near the centreline of spray were more homogeneous than at the edges of the sprays, Yule et al. [1].

To heat the rotating disk, six specially manufactured propane-oxygen "surface mix surface tube" (SMST) burners manufactured by "Nordsea Gas Technology Ltd" (NGT) are used, as described previously in [2]. The burners can be moved nearer to or further from the surface (10 to 50 *mm*) and also from side to side.

Water was supplied by the high-pressure plunger pump (type: NP25/50-120, manufactured by Speck Triplex) via a header tank, and could feed either one or two “UniJet” full cone spray atomisers, depending upon whether both or just one surface of the disk is sprayed. Atomisers used in these experiments were manufactured by “Spraying Systems Co.”. For convenience these atomizers are named as “TG0.5, TG1.0 and TG3.5” with orifice diameters of 094, 1.19 and 1.70 respectively. Here TG and the corresponding numbers (0.5, 1, and 3.5) are the manufacturer’s codes, which relate to tip type and capacity size, respectively. The maximum possible injection pressure was 12.0 *MPa*. Details of the performance of the atomizers are given in Sharief et al. [5] and Nasr et al [2]. The central region of the sprays were selected by using a rectangular slot in the metal canopy, in order to make a relative homogeneous spray zone impact on the surface.

To measure the rapid temperature drop in the transient cooling test under rotating conditions, thermocouples with a slip ring commutator manufactured by "I.D.M Electronics Ltd.", a timer disk and a data acquisition system were used. The timer disk (see Fig 1) with a hole and 126 slots, was specially made for the rig [7] and it was used, not only to measure the speed of the rotating disk, but also to synchronise measurements with position of the instrumented segment of the disk relative to the spray. It is attached to the top of the shaft with two optical signal senders: one is for measuring the disk speed

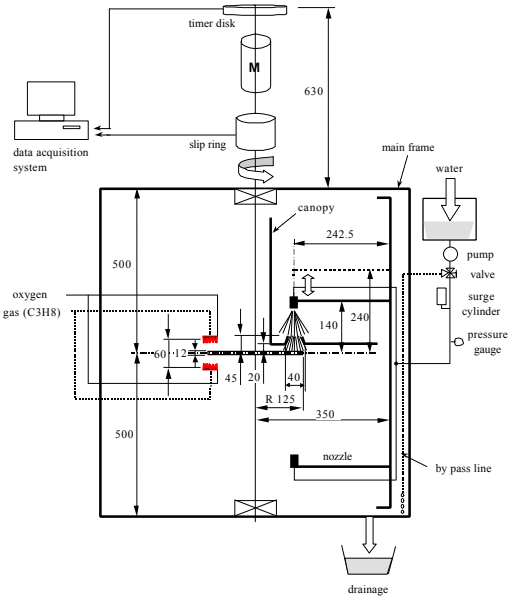

Fig.1 Schematic of transient apparatus

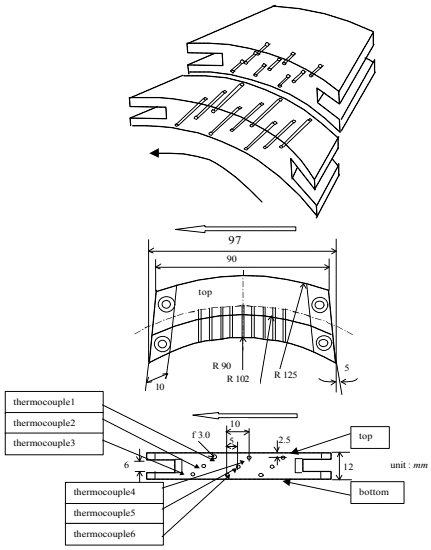

Fig.2 Detail of test segment

and the other is for providing data synchronisation pulses. The speed of the rotating disk was displayed digitally on the speed controller with an accuracy ± 2 *rpm*. The synchronising measurement device sent voltage signals of + 10 *V* to the data acquisition system when the forepart of the test piece passed the vertical centreline of the nozzle exit. The slot in the timer disk was actually 120° in advance of the test piece at that time due to space restrictions for its installation. The pulse time durations of the slot were 0.01 and 0.02 *s* for 120 and 60 *rpm,* respectively. The data acquisition system, which consisted of a Pentium PC and an ADC and an amplifier and pre-amplifier, fed by eight preamplifiers (manufactured by Bell & Howell), was used to measure the temperatures. The maximum sampling data rate was 16 *kHz*. The output of the thermocouples could be amplified up to a maximum ± 10 *V* and converted automatically to temperatures by a calibration data file in the computer. This file was created on the basis of calibrated values for the same diameter K-type thermocouple wires as used in the tests, and the "Temperature Reference Unit" manufactured by CP Instruments was used, with an accuracy ± 0.05 °C.

2.3 Test Procedure

Tests were performed with a vertically downward spray impinging on to the rotating test piece. Preliminary tests showed that at rotational speeds much higher than 120 *rpm*, heat transfer rate for higher temperatures became difficult to measure due to signal noise. Thus two rotational speeds were used, 60 and 120 *rpm*. Measurements were made at vertical distances of 140 and 240 *mm* from the atomiser tip to the test segment, using pressure 0.69, 1.39 and 2.07 *MPa*. The segment and the whole disk were heated first, rotating at either 60 or 120 *rpm* without the spray, until all thermocouples registered the initial temperature (to within ± 2 °*C*), where the temperatures used were 200, 300, 400 and 500 °*C*. Also 600 °*C* was used for 60 *rpm* only. When the target temperature was achieved, the burners were switched off and then the spray was turned on. The spray was

not allowed to impact on the test specimen until it had achieved a stable spraying condition. This could be judged by the operator and took at least 10 *s*. A sliding cover was thus used to cover the rectangular slot orifice until the spray reached a steady state and then this was rapidly removed manually, with the data acquisition system being triggered just before this was carried out. As the specimen started to cool the time histories of the temperatures were recorded, as well as the pulse from the optical trigger at the timer disk.

The test segment was polished before starting a test in order to minimise the effects of roughness of the surface Choi and Kang (4, 10). Temperatures of the six thermocouples were recorded for the first traverse of the segment through the spray and, typically, 4 further disk revolutions. Heat fluxes were calculated for the first spray only (i.e. the first rotation of the disk through the spray). The temperatures of the specimen obtained from the three thermocouples numbers 4, 5 and 6 (Fig. 2) in the middle part of test segment were used in all the data analysis. This was because the temperatures of the three thermocouples in the forepart of test segment (numbers 1, 2 and 3 in Fig. 2), were thought to be affected significantly by water penetration of the gap between the test segment and the remainder of the rotating disk.

Although temperatures up to 1000 *°C* were possible, temperatures were restricted to 600 *°C* in these experiments, to ensure that there was no failure of equipment. It is intended that an extension of the project may move to a higher temperature. The rotational speeds of the disk (60 and 120 *rpm*) provided tangential velocities of 0.7 and 1.4 $m\ s^{-1}$, for the centre of the test segment. The velocities, although relatively low, are commonly found in steel-making. The velocities were restricted in these tests, for the same reasons as the restriction of the temperature.

3. Experimental Results and Discussion

In the examples in Fig 3, the temperature-time curves consist of four periods: a "non-spray" period, followed by three transits under the spray.

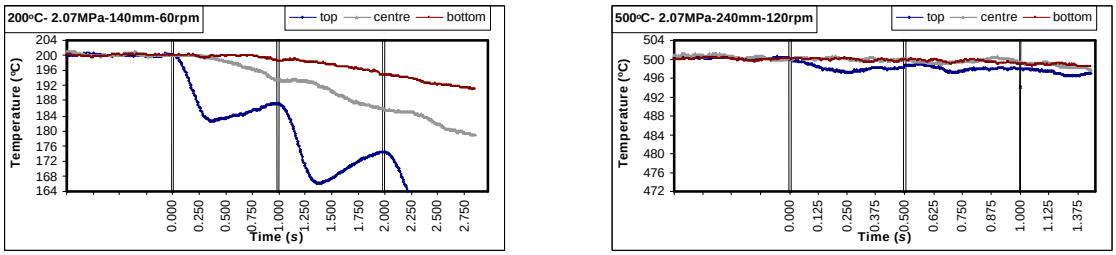

(a) (b)

Fig. 3 Temperature time histories using 1.70mm nozzle at 2.0 MPa, (a) initial temperature 2000 ^{0}C, 60rpm, x=140mm, (b) 500 ^{0}C, 120rpm, x=240

The non-spray period was useful for confirming that thermocouples were operating satisfactorily and that temperature was homogeneous in the test piece to within ±1^{o}C. The temperature at the end of the non-spray period specifies the initial conditions prior to spray cooling. When the forepart of the test piece passed the vertical centerline of the nozzle, the synchronising pulse was used to define "zero time", as shown in Fig 3. There

is a further time interval of 0.05s at 60rpm, and 0.025 at 120rpm, before the centre thermocouple, number 5, is under the spray centreline. Thermocouples 4, 5 and 6 are used in all data that are presented below and they are spaced across the thickness of the test piece segment and are, as shown in Fig 2, nearly in-line through its centre. The signals from the other thermocouples were used to check that the temperature field in the test piece varied significantly in the circumferential and vertical directions only, i.e. two-dimensionality could be assumed as a reasonable approximation (to within $\pm 1^{o}$C). Thermocouple 1, near the cooled surface and near the leading edge of the test piece, tended to give inconsistent readings, caused by leakage of water into the small gap between the test piece and the main annular steel ring. As seen in Fig 3(a), after the relatively constant values in the non-spray zone, the temperature dropped rapidly during and after impaction of the water spray. After the test piece leaves the main cooling area, temperature recovered to some extent (due to heat redistribution in the metal), until entering the next cooling region. The repeated cooling and heat recovering signals are very similar in their patterns, which is an additional check on experimental accuracy.

Figure 3 show the representative temperature-time histories in the "top", "centre" and "bottom" (thermocouples 4, 5 and 6) for two cases near the extremes of cooling rate. These both use a water pressure 2.07MPa, and nozzle diameter, 1.70mm. Figures 3(a) and 3(b) show, respectively, cases with rotating speeds, 60 and 120rpm, surface-nozzle distances, x, 140 and 240mm, and initial temperatures 200 and 500^{o}C. The impacting water mass flux for case (b) is less than half that for case (a), as shown in Table 1. The effect of different surface-nozzle distances, on the cooling rate of a test piece has been studied by [8], for stationary surfaces. Case (a) is near the expected critical (peak) cooling rate, Sharief [5], on the boundary of the nucleate and mixed cooling regimes, whilst case (b) is in the film regime. Naruhito et al [11] concluded that, what they called, the "quenching point" (the Leidenfrost point) occurred in the temperature range between 230-240^{o}C, in their experimental results. The temperatures from 300^{o}C to 600^{o}C in the present experiments can be regarded as being the film boiling regime.

It is clear that in the case in Fig 3(b), the temperature drop per revolution is comparable with temperature fluctuation occurring within one revolution. However fluctuations of this magnitude are not observed in the case shown in Fig 3(a). Thus their occurrence in case (b) is likely to show real variations in cooling rate with time that are occurring in the film regime. The lower temperature drop at thermocouple position 4, at the higher rotational speed 120rpm, is also attributed to the reduced residence time of the spray at any part of the surface. Naruhito [11] and Chen et al [12] experienced the adverse effect on cooling of the speed of a cooled object. Considering Fig 3(a), the temperature at position 4, which lies near the surface, drops rapidly after impaction of the first water spray, and reaches a minimum before it recovers relatively slowly, by means of heat redistribution from the lower part of the test piece, until the segment enters the next cooling stage, giving repeated cooling and heat recovering. Temperatures in the central part of the test piece (i.e. thermocouple 5) generally maintain mid-range temperatures between top and bottom thermocouple positions, without rapid temperature drops. For the case in Fig 3(b) there are occasional cross-overs of measurements at the central and bottom positions (thermocouples 5 and 6). Temperatures in the bottom part of test piece (thermocouple 6) are observed to decay nearly monotonically, with no sign of transient cooling as the top surface passes through the spray.

It is recalled that to minimise temperature distortion within the test piece, the thermocouples were staggered in their positions. The phase differences at 60rpm due to stagger were 0.007s, both between thermocouples 4 and 5, also between thermocouples 5 and 6, and half this time at 120rpm. The data files have not been corrected for these phase differences because they are small relative to the time scales of temperature variations.

From the general results obtained, for which Fig.3 represents just two examples, temperature-time curves display relatively repetitive curves of the cooling and restoring process in and after the spray zones. The present study focused on the first spray zone for which the spray impacted upon a dry, vapour-free surface with uniform temperature across the test piece. Figure 4 shows typical temperature time histories at the top position (thermocouple 4) during this "first spray", with mass flux, G, values 1.86, 5.59, 9.89 and 12.50kgm^{-2}s^{-1}. These are for in Fig 4(a), 200^{o}C temperature at 60rpm, and for Fig 4(b), 500^{o}C at 120rpm. The spray cases used here may be deduced from Table 1 where it can be seen that droplet velocity and diameter are also changing from case to case. Thus care must be taken when interpreting results, such as those in Fig 4, in terms of the effect of one parameter. Deconvolution of the effects of the different parameters requires correlation procedures, as discussed below. However, in agreement with work using stationary surfaces, the mass flux G is in fact the most important parameter in determining cooling rate.

It is noted that the actual surface temperature in the region of direct contact with the water spray, should be lower than at the top thermocouple position of the test piece, because the active junction of thermocouple 4 was welded 2.5mm under on the surface however it is not necessary for present purposes where only the initial surface temperature is specified as a parameter and this does not suffer from this error source. A correction could be made, if required, by extrapolating the measurements at positions 4 reductions increase with increasing mass flux and 5, to the surface.

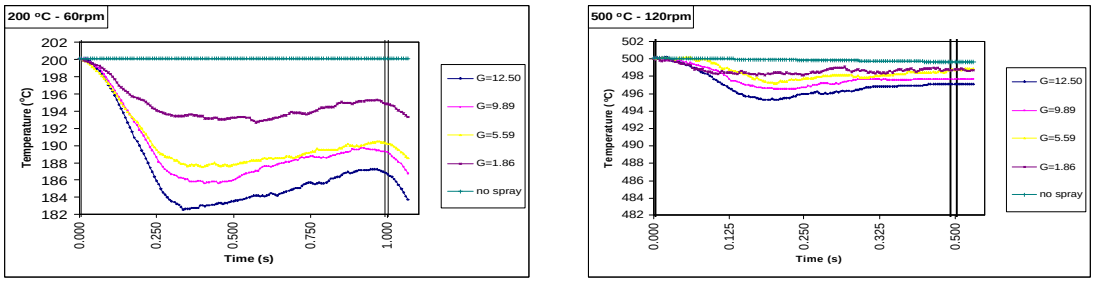

(a) (b)

Fig. 4 Surface temperature time histories at four different mass fluxes, G (kgm^{-2} S ^{1}), at (a) 200 ^{0}C with rotating disk at 60rpm, and at 500^{0}C at 120rpm

Table 2 Temperature reductions for one disk revolution without water spray

Initial disk Temperature	200 ^{o}C	300 ^{o}C	400 ^{o}C	500 ^{o}C	600 ^{o}C
60 rpm	negligible	0.1	0.3	0.8	1.0
120 rpm	negligible	0.4	0.5	0.9	Not used

In all cases the temperature confirming that the mass flux is one of the main parameters determining heat transfer in both transition and film regimes. The temperature-time curves without a spray, obtained with the disk speeds 60 and 120rpm, are also shown in 4. These temperature reduction rates, are due to radiation, air convection and conduction to the supports. The temperature reductions for one disk revolution without spraying, are shown in Table 2. These reductions are small compared with those due to the spray cooling, particularly at the lower temperatures. However they are taken into account in the spray cooling heat flux calculations, as described later.
In summary, after the higher frequency noise had been filtered out, the temperature signals obtained for different spraying conditions were deemed to be repetitive and self-consistent and their use for heat transfer calculations is justified.

3.1 Local Heat Flux

One-dimensional heat flux calculation procedure was used for estimating the local heat flux from the surface.
As sketched in Fig 5, to calculate the evaporative heat flux at the surface of the rotating test piece, the test piece is represented by an infinitive plate, which moves with a velocity which is that of the tangential velocity of the centre of the test segment. This velocity is $V = 2p? R,$ where the radial position of the centre of the test segment is at $R = 0.1075$ *m* and *?* is the rotational speed (revolutions per second). The local "evaporative heat flux" can therefore be represented as: $q^o = ?DC_p\ d/dt\ (T_{nospray} - T_{ave})$ (W/m^2). The average temperature, T_{av}, for the thickness of the test segment was calculated; using a quadratic fit the three measured temperature values.

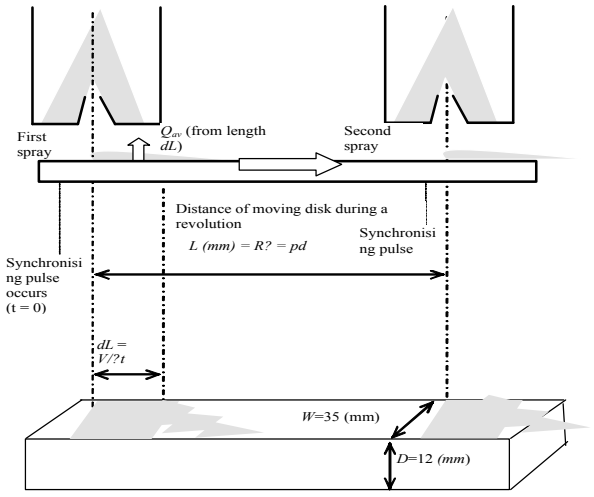

Fig. 5 Schematic diagram for heat flux calculation

The equation assumes that temperature does not vary radially across the test segment. Subtracting the segment temperature measured without spraying, $T_{no\ spray}$, is a means of correcting for radiative heat transfer although it is also removing heat transfer to the air, for the non-spraying case. Results are shown in Figs 6 for the three full cone atomisers [1] at different conditions. Note that the synchronisation pulses shown in the graphs represent the points where the forepart of the segment passed under the spray centre-line.

The position of the spray centre-line is at L = 21.5 *mm*, for both 60 and 120 *rpm*. Figures 6(a) shows the heat flux curves for 200 °*C* (± 1 °*C*) initial surface temperature, for three atomizers operating at 2.07 MPa, for nozzle-surface distance 140mm, at 120rpm. Due to the differentiation of the temperature time histories required to obtain heat flux, there is more scatter in the curves than for the temperature time histories shown in Fig 4. The levels of heat flux are seen to increase as the atomizer size is increased with its consequent increase in spray mass flux (Table 1), and peak heat fluxes around 1.5Wk/m^{-2} are shown.

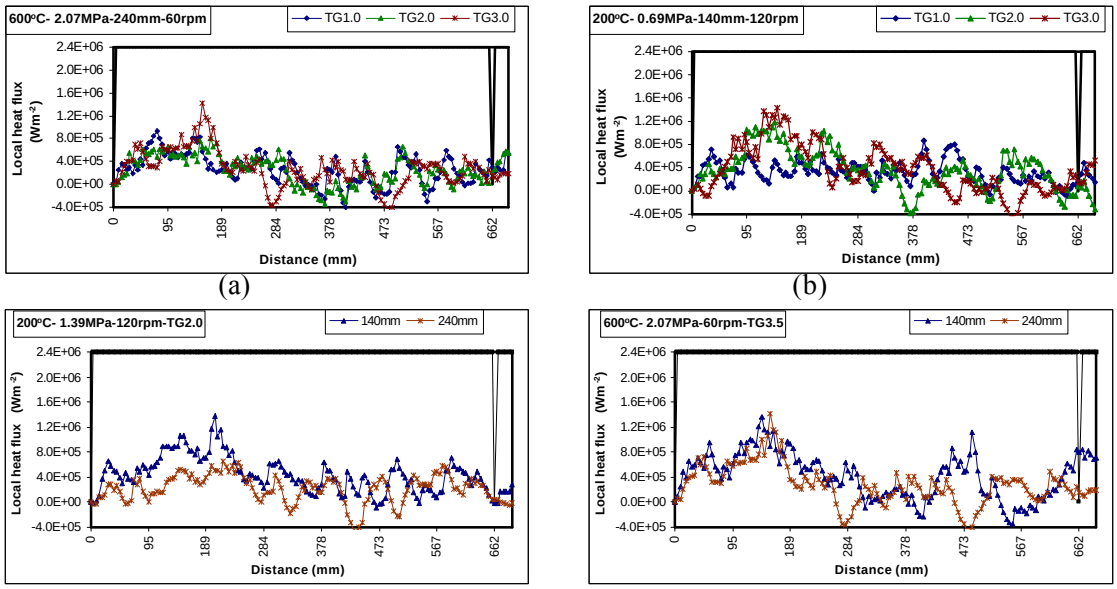

Fig. 6 Surface heat flux at temperature of 200 ^{0}C and 600 ^{0}C for different conditions

Because the relatively low heat flux at 600°*C* at the higher rotational speed was found to be "drowned" by the scatter in the results, the 600°*C* cases were recorded and processed for nozzle-surface distances at 60rpm only, as shown in Fig. 6(b). Figure 6(b) shows similar trends for the cases in Fig 6(a), but with lower heat flux, as expected in the film boiling regime. Figure 6(c) shows cases for one atomizer with a lower water pressure than the cases in (a) and (b), and with two atomizer-surface distances. This shows the increasing problems due to scatter in the data as mass flux is reduced, which occurs both when pressure is reduced and also when the distance between the atomizer and the surface is increased [1]. Situations and regions where scatter, due to signal noise, is unacceptable are indicated by regions of, unrealistic, negative excursions of heat flux. Figure 6(d) shows that increasing atomizer-surface separation at 600^{o}C, also introduces significantly poorer signal to noise ratio, at distances beyond the region of peak heat flux. In general, local heat flux increases moving from the centre-line of the impacting spray. For the 60rpm case, peak heat flux occurs in the region 80±20mm downstream of the spray centre-line. This increases to 150±20mm downstream for the 120rpm case. [8] and Raudensky et al [9] found heat flux, for stationary plates, is highest in the stagnation zone at the spray centre-line. It is thus tempting to assume a near linear increase in distance downstream to peak heat flux, as the velocity of the surface is increased. However this

may be too simplistic an assumption to be made, because of the restricted velocities and spray types that could be used.

Although the scatter in the results becomes important at lower heat fluxes and, in particular, results in unrealistic negative values in places, the trends of heat flux are qualitatively as expected. This is particularly true for the first 90° of rotation, i.e. up to a distance 165mm. Of course, with increasing angle the situation deviates increasingly from the case of a spray impacting on a flat rectangular plate with linear motion. Generally, within the first 90^o of rotation, heat flux increases with increasing nozzle orifice size, increasing supply pressure, and decreasing nozzle-surface separation. In addition, heat flux decreases significantly with increased rotational speed. Perhaps the most surprising characteristic is both the delay in the occurrence of the peak heat flux, beyond the main impaction zone of the spray, and, for some cases, the persistence of significant heat transfer to the spray beyond 300mm, that is when the surface has moved 180^o away from the impaction zone.To some extent this is expected from the observations of Raudensky et al. [9] who showed the persistence of cooling to surface vapour and water far from the impaction zone. As shown in Table 1, spray characteristics of the central zones of full cone nozzles are functions of supply pressure (P), exit orifice diameter of atomiser (d_o) and atomiser-surface distance (x). When the distance from the atomiser exit to the heated surface is increased, all of the three parameters, mass flux (G), impinging velocity (U) and drop median diameter ($D_{v0.5}$), are decreased. It is observed in Fig 6 that when the surface-nozzle distance is 140 *mm*, heat fluxes are relatively higher than those for the surface-distance, 240mm. The difference is clear for all nozzle pressures, at 200°C, but is more pronounced for the higher pressure (2.07MPa) for 300, 400 and 500°C. The differences are less clear for 600°C, but this is possibly because they are hidden by the greater relative importance of scatter in the data. Most authors agree that mass flux is the main parameter affecting heat flux, at least for the case of a stationary surface. Fry [8] mentioned that the heat transfer coefficient increased linearly with increasing surface temperature, decreasing nozzle "stand-off" distance and increasing flow rate. Although the results of the present research confirm that the heat fluxes are decreasing with increasing nozzle-surface distance, a linear increase of heat transfer coefficient (as opposed to heat flux) with temperature is not apparent from inspection of the data.

The effects of mass flux, G, median droplet diameter, $D_{v0.5}$, and mean droplet velocity U, cannot be easily discriminated by visual inspection of the data. This requires applying correlation methods and maximum values of heat flux are chosen to elucidate relationships. Figure 7 shows the maximum heat flux plotted against individual spray characteristics for the 200°C case, however, as has been described, great care must be taken when examining Fig. 7, because it was impossible to vary one parameter at a time. The clearest correlation (i.e. with least scatter) is that between maximum heat flux and mass flux. This confirms the importance of mass flux in determining heat transfer. The polynomial trend lines also demonstrate the important effect of the rotating speed of the surface. Otherwise, nothing conclusive emerges from the data presented in this way. The ranges of maximum heat flux are from 4.0×10^5 to $2.6\times10^6 Wm^{-2}$ for the speed of rotating disk 60rpm, and from 4.8×10^5 to 1.6×10^6 W m^{-2} for 120rpm. Maximum heat fluxes in the film boiling regime, in the range of temperature 300 to 600°C, are significantly lower in comparison with the transition regime.

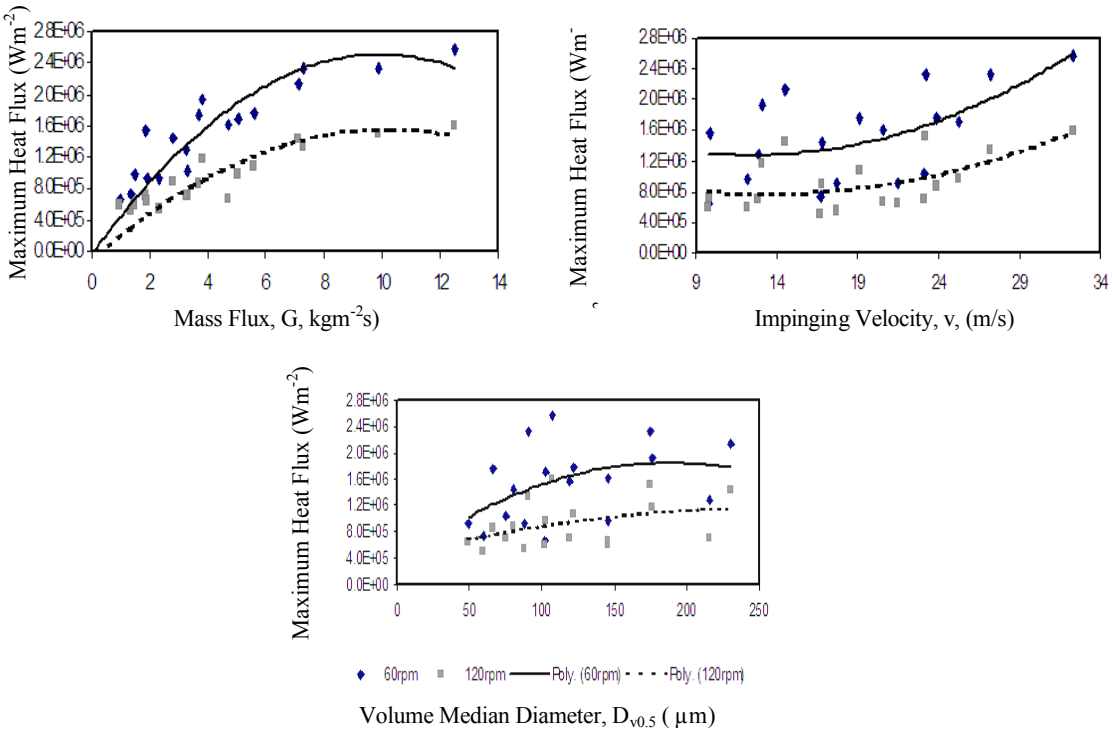

Fig.7 Effect of spray characteristics on maximum heat flux at temperature 200 °C (G, and $D_{v0.5}$ were not varied independently of each other)

The ranges of maximum heat flux in the film boiling regime are from 4.0×10^5 to 1.4×10^6 Wm^{-2} with the speed of rotating disk 60rpm and from 4.8×10^5 to 1.1×10^6 Wm^{-2} with 120rpm. These various ranges are all within the range of values found in previous work on spray cooling of stationary surfaces.

Empirical correlations for maximum local heat flux, $q^{\cdot}_{wmax}(Wm^{-2})$, were obtained using "Microsoft Excel" software and by using experimental data covering a ranges of spray parameters, 0.98 to 12.50kgm^{-2} s^{-1} for mass flux G, 49.0 to 230.4µm, for volume median drop diameter $D_{v0.5}$, and 9.8 to 32.3$m\ s^{-1}$ for average drop impinging velocity U.

The optimum curve fit was obtained for the maximum heat flux, equated to products of G, $D_{v0.5}$, U, and surface superheat DT_e, raised to different powers. For the 60rpm cases the best fit was, in SI units for G, U and DT_e, but using µm for $D_{v0.5}$:

$$\dot{q}_{wmax60rpm}=2.0\times10^6 G^{0.231}U^{0.274}D_{v0.5}^{0.176}\Delta T_e^{0.490} \qquad [1]$$

For the 120rpm cases the best fit was:

$$\dot{q}_{wmax120rpm}=8.0\times10^5 G^{0.192}U^{0.191}D_{v0.5}^{0.046}\Delta T_e^{0.195} \qquad [2]$$

Whilst recognising that such equations are not dimensionally correct, they are very useful in revealing features of the physics of the flows, as is described below.

The top two scatter diagrams in Fig. 8 compare the measured values of $\dot{q}_{w\max,60rpm}$ and $\dot{q}_{w\max,120rpm}$, with values calculated from equations [1] and [2]. It is noted that the full temperature range of results is used for calculating the correlations, i.e. 100°C $=DT_e$=500°C, and thus the use of a single power for T_e is a simplification in view of the different cooling regimes that are covered by the data. This is a reason for the relatively high scatter in Fig 8. For both cases maximum heat flux increases with increasing mass flux, *G* and impinging velocity, *U*, each raised to similar powers. This is interesting because the product GU is the droplet momentum flux at the surface. Thus the results are indicative of relationships between Nusselt and Reynolds number, both suitably defined using spray parameters. Retrospectively this may appear to be unsurprising, yet it is not a concept that has been raised in previous published work. The powers in equations [1] and [2], show that the values of spray parameters and superheat have less influence on maximum heat flux for the lower speed of the test piece. This was not obvious from examining the "raw data" results, thus showing the usefulness of such correlations. An explanation is that as the surface speed is increased, the relative velocity between the wall spray and the surface reduces, and it is likely that a thicker water layer at the surface results so that there is less dependency of heat transfer on the spray properties.

From equations [1] and [2], the drop size has the smallest effect on heat transfer, in agreement with previous work with stationary surfaces. Thus the maximum heat flux was again correlated, but dropping $D_{v0.5}$ from the equation and adding the tangential speed of the test piece *V*. It is noted that *V* could not be used with all of the other four parameters to obtain a single correlation, due to lack of convergence of the iterative procedure. For the 60 rpm and 120 rpm data combined, the best fit was:

$$\dot{q}_{w\max}=2.0\times10^{6}\,G^{0.268}U^{0.215}V^{-0.431}\Delta T_e^{-0.344} \qquad [3]$$

The bottom scatter diagram in Fig. 8 shows the fit of this correlation. From equation [3] the main result is the confirmation that the speed of the surface very significantly affects the maximum spray cooling heat flux. An obvious drawback of equation [3] is that it is inapplicable when *V* ? 0. It is interesting to compare the effects of spray characteristics with those for steady state cooling of a stationary test piece. Sharief et al. (2000) derived a correlation equation, showing that the total heat flux had 0.363 and 0.304 power dependency on the liquid mass flux and drop impinging velocity, respectively, in the surface superheat temperature range between 152 and 630°*C*, using the range of spray parameters: 0.23 to 3.32 $kg\,m^{-2}\,s^{-1}$, 34.71 to 127.99μm, and 7.05 to 23.10 $m\,s^{-1}$.

Thus comparison with the results from the present equations confirms that the effect of mass flux and impinging velocity can be combined as a spray momentum flux and this parameter tends to be more important for reduction in surface velocity. However the heat fluxes measured by Sharief [5], although in agreement with previous experiments cooling stationary surfaces, are lower than the peak heat fluxes that are reported here. This can be seen by the curve included in Fig. 7. This difference is probably due to the heat transfer for the stationary case, being measured at a stagnation zone, whilst the present results show that peak heat transfer occurs downstream of the main impaction zone.

4. CONCLUSIONS

A novel rotating disk technique has been proved a convenient method for determining moving surface heat transfer. The data are consistent however care is required in interpreting the rotating surface results in terms of linearly moving plates, especially beyond 90° of rotation. Unlike for cooling of stationary surfaces local heat flux increases moving downstream from the zone of impaction of the spray, and reaches a maximum at a position downstream that increases as the surface speed is increased. The heat fluxes at a temperature 200°C, in the transition regime, are higher than at temperatures (300°C - 600°C) in the film boiling regime for the moving surfaces.

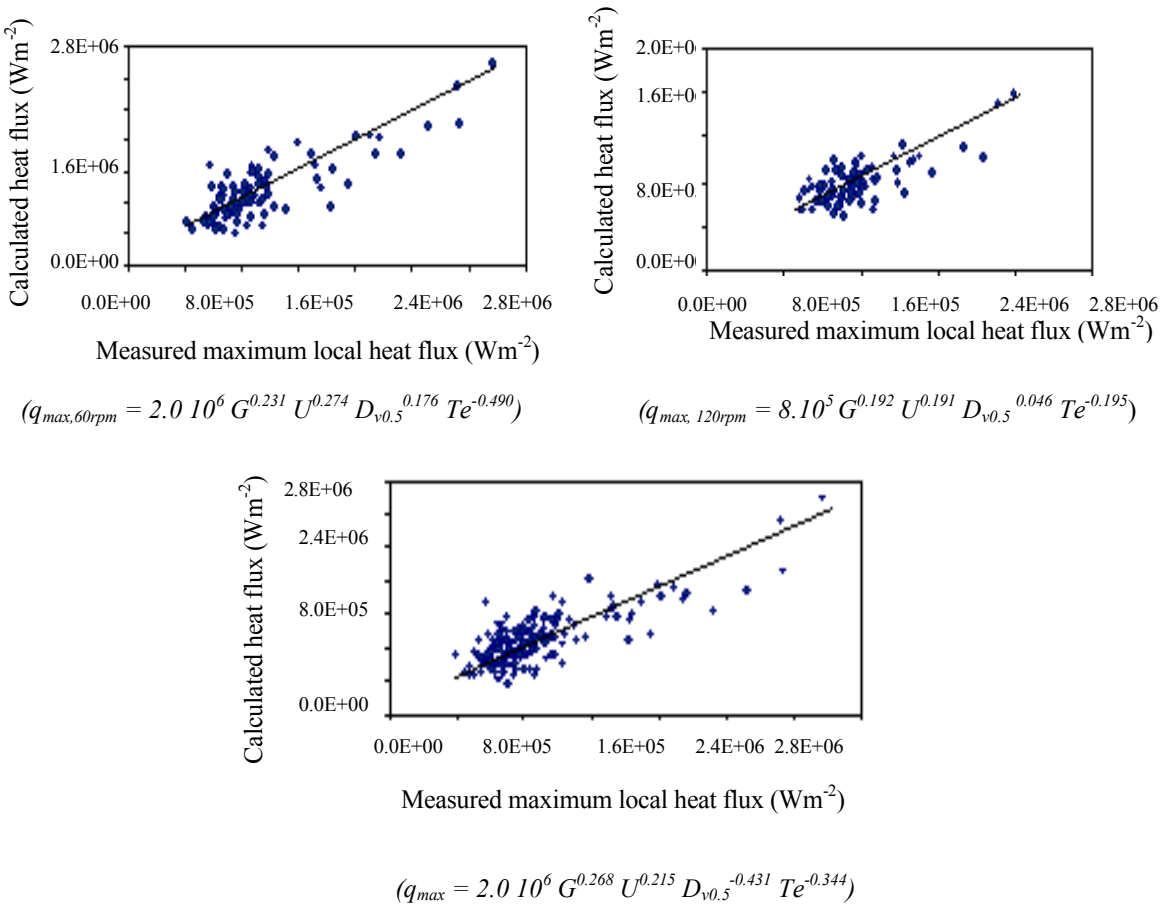

Fig. 8 Comparison of the measured maximum local heat flux with the heat flux from the correlation equations 1, 2 and 3)

Heat flux generally increases with increasing nozzle orifice size, increasing supply pressure, and decreasing nozzle-surface separation. Correlations shows that maximum heat flux increases with increasing mass flux, G and impinging velocity, U raised to similar powers, indicating the importance of droplet momentum flux. The size effects of mass flux, impinging velocity droplet and temperature, tend to be more significant for reduction of surface velocity.

5. References

[1] Yule A J, Nasr G G, and Sharief R A, *The performance characteristics of solid cone spray pressure swirl atomizers*, Atomization and Sprays J., Vol. 10, No.6, pp627-646, Dec 2000.

[2] Nasr G G, Sharief R A, Yule A J, James D D, Widger I R, and Jeong J R, *Transient high pressure spray cooling of a rotating steel plate at high temperature*, Proceedings of 15th ILASS Europe, Toulouse, France, July 1999.

[3] Nasr G G, Yule A J , and Bendig L , *Industrial Sprays and Atomization: Design, Analysis and Applications*, Springer Verlag , June 2002.

[4] Choi K J and Kang B S , *Parametric studies of droplet wall direct heat transfer in spray cooling process*, ASME FED-Vol. 178/HDT-Vol.270, Fluid Mechanics and Heat Transfer in Sprays, pp. 161-165, 1993.

[5] Sharief R A , Nasr G G , Yule A J , James D D , Widger I R , and Jeong J R , *Steady state high pressure spray cooling of high temperature steel surfaces*, Proceedings of 8th ICLASS Conference, Jet Propulsion Lab., Pasadena, CA, USA, July 2000.

[6] Yule A J and Dunkley J J, *Atomization of Melts,* Oxford university Press, 1994.

[7] Rho S, *Water spray cooling of moving heated steel surfaces*, MPhil Thesis, UMIST, Manchester, UK, March 2001.

[8] Fry J C, *A study of the cooling effect of water sprays on steel strip at high temperatures*, EngDoc thesis, Dept. of Mech. Eng., University of Wales, Swansea, 1998.

[9] Raudensky M, Druckmuller M, and Horsky J, *Inverse heat conduction problems and generalization of experimental results*, HTD-Vol. 361-5, Proceedings of the ASME Heat Transfer Division Vol. 5, HSME, pp. 65-71, 1998.

[10] Sabry, T I., Mousa M and Yoshida H, *Studies on the spray cooling of hot surfaces*, ICLASS-'94, Rouen, France, Begell House NY, pp. 891898, July 1994.

[11] Naruhito S, Hariki M., Haraguchi Y and Morita M., *Mechanism of uneven thermal distribution formation during water cooling at low temperature for a moving plate*, ISIJ, Tetsu-to Hagane, Vol. 86, No.6, pp 381-387, 2000

[12] Chen S J., and Tseng A A, *Spray cooling and jet cooling in steel rolling*, Int. J. Heat and Fluid Flow, Vol. 13, No. 4, pp358-369, Dec. 1992.